

A Measurement of the Flux of Cosmic Ray Iron at 5×10^{13} eV

J. Clem¹, W. Droege^{1,2}, P.A. Evenson^{1,3}, H. Fischer², G. Green², D. Huber¹, H. Kunow², and D. Seckel¹

ABSTRACT

We present results from the initial flight of our Balloon Air Cherenkov (BACH) payload. BACH detects air Cherenkov radiation from cosmic ray nuclei as coincident flashes in two optical modules. The flight (dubbed PDQ BACH) took place on April 22, 1998 from Ft. Sumner, New Mexico. During an exposure of 2.75 hours, with a typical threshold energy for iron nuclei of 2.2×10^{13} eV, we observed several events cleanly identifiable as iron group nuclei. Analysis of the data yields a new flux measurement that is fully consistent with that reported by other investigations.

1. Introduction

It is important to extend direct measurements of cosmic ray composition towards the knee of the cosmic ray spectrum. Determining composition in this region is one of the keys to understanding cosmic ray acceleration and propagation. Air shower techniques are a potential tool for measuring composition at the knee, but their interpretation ultimately relies on extrapolation of particle interaction models to regimes not directly tested in laboratory experiments. Emulsion techniques and electronic detectors must be improved before they can provide an independent calibration of air shower experiments, and so the potential for systematic error exists. We have designed an experiment (Evenson and Seckel 1995; Seckel et al. 1999) to determine the flux of iron nuclei at energies between 3.0×10^{13} and 3.0×10^{14} eV by detecting atmospheric Cherenkov radiation from the incoming nucleus before it undergoes a nuclear interaction. By achieving an absolute measurement of the iron flux, relatively free of the uncertainty in particle interaction models, the Balloon Air Cherenkov (BACH) technique can provide an independent calibration for air shower experiments, thus opening a path for composition measurements for energies at and above the knee. This technique was discussed by Sitte (1965) and Gough (1975), and used initially by Sood (1983; Sood and Panettieri, 1981). In this paper we report the result obtained from the initial flight of our developmental balloon payload (PDQ BACH).

¹Bartol Research Institute, University of Delaware, Newark, DE 19716

²Christian-Albrechts-Universität Kiel, D-24089 Kiel, Germany

³National Science Foundation, Arlington, VA 22230, USA

2. Technique

A high energy iron nucleus entering the atmosphere has an interaction length of 13.2 gm/cm^2 (Hufner 1985). Before interacting, a sufficiently high energy nucleus will begin to radiate photons via the Cherenkov process. These photons travel close to the primary particle, forming a “light pool” whose characteristics can be calculated from elementary considerations and knowledge of the density profile of the atmosphere. Figure 1 illustrates the radial profile of the light pool for a variety of particle energies and nuclei. At 35 km altitude, attainable by a NASA balloon, the diameter of the lightpool increases from zero at the threshold energy to a maximum of about 15 meters for a fully relativistic particle incident 45 degrees from the zenith. The intensity has a central peak, a cusp at the edge of the pool, and a broad floor at intermediate radii. For an iron nucleus the floor is about 2000 photons per square meter in the spectral band from 0.3 to 0.6 microns. With finite size light collectors the peak and cusp are softened, and for the 24.3 cm radius light collectors employed by PDQ BACH the floor corresponds to about 400 photons. Quantum efficiency of our system is about 0.1, so a minimum of 40 photoelectrons are detected in each collector. These arrive with a time spread of less than 0.1 ns and produce a single pulse when observed by a photomultiplier tube. The trigger resolving time of the instrument is determined by the approximate 4 ns pulse width of the photomultipliers.

Cherenkov flashes from iron must be detected against the night sky background light. Fluctuations in response to background light can cause false event triggers reducing live time of the instrument, and sufficiently strong fluctuations may be confused with signals from cosmic ray iron nuclei. The PDQ BACH telemetry system takes 0.78 seconds to readout one event. To achieve livetime of 90% we must limit the background trigger rate to 0.1 Hz. This means that the false trigger probability should be less than 4×10^{-10} per resolving time. Operating two collectors in coincidence allows a fluctuation trigger rate $P = 2 \times 10^{-5}$ per resolving time in each collector.

The mean number of background photoelectrons in one sample is $N_B = \epsilon \phi_B A \Omega t$, where ϵ is the detection efficiency, ϕ_B is the background flux, A is the collector area, Ω is the solid angle, and t is the integration time. Pre-flight, we anticipated a dark sky background of $10^8 \text{ cm}^{-2} \text{ sr}^{-1} \text{ s}^{-1}$, which corresponds to $N_B \approx 4$ photoelectrons for BACH’s design parameters. For this N_B , a single collector threshold of 14 detected photoelectrons yields $P = 10^{-5}$. The equivalent photon count is shown in Figure 1 as the horizontal line labeled “P5”. For $N_B = 8$ the corresponding threshold rises to 22 photoelectrons. During flight, N_B varied between 6 and 8 photoelectrons, with occasional excursions as bright stars came into the field of view. At 40 photoelectrons, cosmic ray iron events lie well above the thresholds of 14-22 photoelectrons required from deadtime consideration. The fluctuations themselves are on the tail of a steep distribution, so an increase in threshold by a modest $\sim 15\%$ in post-flight analysis lowers the effective background rate to less than one per hour and allows for a clean separation of fluctuations and cosmic ray events.

Lower Z nuclei may be confused with iron if the cusp or central peak of the light pool falls on a collector. By separating the two coincident detectors by $\sim 3 \text{ m}$ one may ensure that the central

peak cannot simultaneously overlay the two collectors, thus largely eliminating the background from low Z nuclei. The cusps for CNO nuclei are not strong enough to generate triggers, but silicon events where the cusp falls on both collectors may mimic iron. As an illustration of the characteristics of the BACH instrument, Figure 2 shows the results of exposing a numerical model of the instrument to a simulated flux of cosmic rays. Panel (a) shows that silicon may provide some contamination for low intensity iron events, while panel (b) demonstrates that CNO nuclei do not. Details of the model are given in Section V.

We also considered other sources of background, such as Cherenkov radiation from 10 GeV electrons entering a collector (~ 50 photons) and 100 GeV iron nuclei generating fluorescent radiation directly in front of the collectors (~ 10 photons), but neither has enough intensity to trigger the instrument. Numerous lower energy charged particles may pass through a detector generating spurious signals. By running two collectors in coincidence, the trigger rate from such processes is diminished. Offline analysis can distinguish between the few remaining particle events and true cosmic ray events.

In evaluating the viability of the BACH technique one must also consider details of the atmospheric density profile and factors that could alter the assumed straight line trajectory of the radiating nucleus. We assume a US standard atmosphere (NOAA 1976) profile with the density normalized to match the density of the atmosphere at the pressure altitude of the balloon. We have not modeled absorption due to ozone as the edge of that feature is obscured by absorption in the optical components of the instrument. We considered deflection by multiple Coulomb scattering and hadronic interactions (both 10^{-5} radians), as well as magnetic bending which may be a factor 5 larger depending on the track geometry. These effects are significantly smaller than 10^{-3} radians, the Cherenkov angle at altitude for fully relativistic particles, and so have not been included in our simulations of the experiment. Hadronic interactions eventually disintegrate the primary nucleus; however, most of these interactions are soft. Disintegration takes several interaction lengths and occurs mostly after the primary has passed the balloon. We estimate a 9% exposure correction for this process, but do not model it in detail.

3. Instrumentation

Our payload is illustrated schematically in Figure 3. Given the intrinsic 100 psec duration of the Cherenkov light flash, the primary approach to skylight background is to reduce signal integration time. To this end, we employ Hamamatsu R4143 three inch diameter photomultipliers with a risetime of 2.4 nanoseconds at our operating point of 1200V. We also reduce background by limiting the acceptance aperture with light collectors (208.8 cm long, 24.3 cm radius aperture) based on concepts developed by Winston and colleagues (Welford and Winston 1989). These collectors have a nearly flat response within a well defined 7.5 degree half angle field of view. To reduce backgrounds, two collectors, separated on axis by 2.87 m, were operated in coincidence. The Winston collectors for PDQ BACH were constructed using a precision-machined aluminum

mandrel. Each collector consisted of two upper and two lower sections, molded individually on the mandrel from carbon fiber epoxy composite material. A reflective aluminum coating was evaporated onto the sections, which were then assembled.

Photomultipliers attached to the collectors must operate in the presence of a comparatively high DC current from starlight, which must be monitored accurately while still maintaining satisfactory high frequency response. By operating with negative high voltage, the anode current can be directly measured; however, a photocathode (and, consequently, photomultiplier faceplate) maintained at negative high voltage while exposed to low atmospheric pressure poses an unacceptable risk of corona discharge. Our solution was to construct Pressurized Optical Detectors (PODs), as illustrated in Figure 4, to operate the photomultipliers at one atmosphere, and couple them to the collectors via light pipes of Bicron UV transparent acrylic. The light pipes extend out from the PODs to allow thermal isolation of the PODs and collectors, while providing electrical insulation as well. Surfaces of each light pipe are polished and kept from contacting the POD structure except for a 0.32 cm tapered flange that provides a pressure seal. Each light pipe is internally reflecting for almost all signal photon trajectories. The PODs also contain R329 photomultipliers coupled to plastic scintillators that cover the detector photomultipliers and internal sections of the light pipes to serve as an anticoincidence shield against cosmic rays. Each photomultiplier receives high voltage from an individual power supply, adjustable in flight.

Data were acquired with a Tektronics TDS640A digital oscilloscope which flew as part of the payload. This oscilloscope captures 2 gigasamples per second in four channels simultaneously. The four channels were used to record data from the two R4143 photomultipliers (denoted C1 and C2) and the two anticoincidence detectors (A1 and A2). Internal oscilloscope logic was used to detect coincident triggers where the signals in C1 and C2 both exceed thresholds. The thresholds were independently adjustable during flight. The anticoincidence channels were not part of the trigger, but were used in off line analysis. The TDS640A comes equipped with a GPIB interface, so we developed a microcontroller-based unit to interface it to the command and telemetry system.

Crucial to the scientific return of a BACH payload is calibration of photomultiplier gain, pulse shape, and the efficiency of the light collectors. The full optical assemblies were calibrated for angular efficiency and alignment within the Ft. Sumner hanger (Seckel, et al 1999). A 2.54 cm diameter diffuse light source was moved horizontally and vertically across the field of view at a distance of 7.5 m from the front of the collectors. The results of these tests were interpreted with the aid of ray tracing models for the collectors/PODs. The models include losses due to reflection from the collector (4%), absorption by the aluminum coating (20%), absorption in the light pipe (12%), losses from the optical path (4%), and yield an overall collector efficiency of 0.60 for a head on Cherenkov spectrum weighted by the photomultiplier quantum efficiency. Off axis, performance drops near the edge of the field of view in a calculable and testable manner. Minor adjustments were made to the individual collector models based on the test results. The adjusted models for the individual collectors were then used to determine instrument response to a light source at infinity.

Calibration of the photomultiplier response was complicated by low gain at the flight voltage of 1200 V and an inability to resolve pulses from single photoelectrons. We therefore followed a multistep process including determination of the absolute single photoelectron response at high voltage (2150 V), the relative gain curve from 2150 V down to 1200 V, and a comparison of charge and pulse height response at 1200 V. The mean pulse height per photoelectron for strong pulses at flight voltage was 0.24 mV/pe in collector C1 and 0.19 mV/pe in collector C2. Single photoelectron pulse height distributions were determined at high voltage and extrapolated down to flight voltage using an 8 stage model for the R4143 photomultipliers.

Ground level observations of cosmic rays provided a check on the absolute normalization of the collector and POD response. Muons passing through the light pipe serve as a rough check of the light pipe model and photomultiplier gain. Similarly, we are able to measure Cherenkov light from ground level muons and electrons passing through the collector volume on trajectories nearly parallel to the optical axis. We also performed ground level observations of Cherenkov light produced by cosmic ray air showers as a full system check of the payload in flight configuration.

4. Observations

PDQ BACH was launched at sunset from Ft. Sumner, NM, on April 22, 1998 and cut down ~ 6 hours later, yielding a useful exposure of 2.75 hours. Atmospheric pressure during the observation varied from 8.05 to 8.5 mb, corresponding to a threshold energy for iron of 2.2×10^{13} eV. The instrument collected 1793 triggers, each consisting of 250 ns (500 samples) of waveform from four channels: the two collectors and the two anticoincidence detectors. Since the signals resulting from the Cherenkov light are only a few nanoseconds wide, most of the waveform data are available for monitoring the skylight background. Expecting only a handful of true iron events, the trigger thresholds on the detectors were intentionally set to acquire events at a rate of approximately 0.1 Hz to allow detailed study of background sources.

Sample events from flight data are shown in Figure 5. Panel (a) contains one of the events identified as due to an iron nucleus. Note the identical arrival times of the similar sized pulses from the two collectors (C1 and C2) and the absence of signal from either anticoincidence (A1 and A2). Panel (b) shows a trigger with two moderate signals in C1 and C2. On the basis of pulse height, the event could be a silicon nucleus or iron incident at the edge of the field of view; however, there is a 2.5 ns offset in the two pulses, so this event is classified as a rare, high-amplitude skylight fluctuation. Panel (c) shows a typical event where a relativistic particle passes through one of the light pipes accompanied by a skylight fluctuation in the other channel. In addition to the signal in the anticoincidence detector, the event shows asymmetric response and a significant time lag between the C1 and C2 pulses. The time delay between collector (R4143) and anticoincidence (R329) signals results from the different transit times within the two types of photomultiplier. Panel (d) shows a rarer type of background event. The relative timing of the signals indicates that a particle passed through the light pipes and anticoincidence detectors in both of the PODs.

Data from one, 1.75 hour, segment of the flight are shown in Figure 6. This represents the longest exposure taken with unchanged trigger conditions. Data obtained under other sets of trigger conditions were analyzed separately, and the final results were combined. Several events from the 1.75 hour segment have the exact characteristics that we expect from cosmic ray iron nuclei, namely strong coincident sharp signals well above threshold in both channels and no signal in either anticoincidence detector. Of the remainder, the majority have amplitudes just above threshold, and are most likely due to simultaneous fluctuations in the skylight background. As expected, the rate of such triggers is a strong function of the amplitude of the DC current observed in the waveforms outside the pulse region. We observed numerous asymmetric events where C1 records a strong signal and C2 is just above threshold, resulting from charged particles passing through the light pipe in C1 accompanied by statistical fluctuations in C2. The rate of these light pipe events is also consistent with expectations. The relative lack of events where particle hits are evident in C2 coincident with a fluctuation in C1 results from an asymmetry in trigger levels on the oscilloscope. This was intentional, to aid in controlling the trigger rate in a changing background. About 75% of light pipe events are tagged by A1, consistent with our modeling for coverage by the anticoincidence detector. A few events have strong pulses in both channels but are clearly not caused by Cherenkov light, since both anticoincidence detectors also show signals. In all of these cases one signal leads the other by about 10 ns, consistent with a single charged particle passing through both light pipes.

5. Results

After eliminating events with anticoincidence hits, the data can be described as the sum of two distributions characterized by the time separation dt of the two pulses. For true cosmic ray events, the signals arrive within a narrow coincidence window corresponding to the geometry of the collectors ($dt \sim 1$ ns). Skylight fluctuations have a broader distribution corresponding to the pulse width of the photomultipliers ($dt \sim 4$ ns). Events with strong signals are predominantly of the first type, whereas events with smaller signals are mostly in the second. We count cosmic ray events as those with signal greater than 8.5 mV in both channels and $dt < 0.75$ ns. There are 9 such events. Some of these events could be skylight events which just happen to have $dt < 0.75$. By comparing to the clean skylight sample, i.e. events with $dt > 0.75$ ns, we estimate a skylight background count of 0.75 events. We also estimate that inefficiency of the anticoincidence detectors has resulted in false acceptance of 1 event, leaving a total of 7.25 cosmic ray events.

To convert this number to an iron flux, we compare to the mathematical model of the instrument exposed to a flux of cosmic ray nuclei of assumed composition and spectrum, as illustrated in Figure 2. The incident flux is taken to be isotropic over the field of view of the collectors with impact parameters that allow for all positions and orientations of the payload. Knowledge of the light pool, impact parameters, and POD/collector efficiency are combined to yield an expected number of photoelectrons, which in turn is the basis for drawing a signal amplitude from a dis-

tribution based on Poisson statistics, the photomultiplier single photoelectron response and the modeled pulseheight distributions for the photomultipliers. Contribution of background light to the signal is modeled by overlaying livetime weighted randomly chosen sections of waveform from the pre-trigger flight data. Pairs of pulseheights thus determined are displayed in the scatterplots of Figure 2. Applying the 8.5 mV cut to the simulation yields a count which is directly comparable to the 7.25 counts from analysis of the flight data.

Normalizing the exposure to the simulation, yields a flux of $\phi_{Fe}(5.05^{+4.5}_{-1.6} \times 10^4 \text{ GeV}) = 677^{+192}_{-139} E^{-2.5} \text{ m}^{-2} \text{ sr}^{-1} \text{ s}^{-1} \text{ GeV}^{1.5}$. We use Poisson statistics to estimate the statistical error. The energy value (range) is the peak (width at half maximum) of the distribution obtained by convoluting the instrument response with an assumed $E^{-2.5}$ spectrum. The result is reasonably independent of the 8.5 mV analysis threshold, but depends on the assumed iron spectral index. With a small number of events and uncertain calibration we cannot determine the spectrum. Our result also depends on the composition, as silicon nuclei with particular impact parameters can imitate the signals from iron. For the 8.5 mV threshold analysis, the result includes a 6% correction to account for mis-identified silicon. Corrections were also made for hadronic interactions of iron in the atmosphere (estimated 9 %), and for contamination of the iron flux by nuclei with $Z = 17\text{-}25$ (estimated 10%).

Figure 7 compares our new determination of the iron flux with earlier measurements. Our results are consistent with both the CRN and JACEE determinations. All of the recent data are above the flux reported by Sood (1983). We have not reanalyzed Sood’s experiment, but have attempted to improve on his pioneering effort in several ways to make our instrument easier to model and the interpretation of the data more certain.

We thank A. McDermott, L. Piccirillo, E. Rode, C. Scharmberg, L. Shulman and J. Poirier for technical assistance. The collectors were produced in collaboration with the University of Bremen, the Astronomical Institute in Hamburg, and the private firm “Surf Affairs”, located near Kiel. We thank the National Scientific Balloon Facility for the balloon flight and the NSBF staff for preflight assistance. The work was supported in part by NASA grant NAG5-5063 and NAG5-5221.

REFERENCES

- Asakimori, K. et al. 1995, Proc. 24th Int. Cosmic Ray Conf. (Rome) **2**, 707.
- Gough, M. P. 1975, Phys. G. (Nuclear Phys.), **2**, 965-969.
- Evenson, P.A. and D. Seckel 1995, Proc. 24th Int. Cosmic Ray Conf. (Rome) **3**, 583-586.
- Hufner, J., Phys. Reports **125**, 130, 1985
- Sitte, K. 1965, Proc. 9th Intl. Cosmic Ray Conf. (London), **2**, 887

- Seckel, D., et al. 1999, Proc 26th Intl. Cosmic Ray Conf. (Salt Lake City) **3**, 171-174.
- Sood, R. K. and J. Panettieri, NIM,, **185**, 427, 1981.
- Sood, R. K. 1983, Nature, **301**, 44-46.
- Swordy, S. et al. 1993, ApJ, **403**, 658-662
- “U.S. Standard Atmosphere,” NOAA, NASA and USAF, published by the U.S. Government Printing Office, Washington, D.C, 1976
- Welford, W.T., and Winston, R. 1989, *High Collection Non-Imaging Optics*, Academic Press, Inc., San Diego.

Fig. 1.— Yield of Cherenkov photons as a function of distance perpendicular to the primary trajectory (impact parameter) for primaries incident at a zenith angle of 45 deg, a balloon altitude of 35,000 m, and a collector radius of 24.3 cm. The horizontal line labeled “P5” is the signal threshold required to reduce the rate of fluctuation triggers (for two collectors in coincidence) to less than 0.1 Hz under dark sky conditions. Cherenkov flashes from silicon nuclei may be confused with iron for some impact parameters, but an instrument with two collectors separated by 3 meters will never be triggered by oxygen nuclei.

Fig. 2.— Simulated long duration balloon exposure (6 collector pairs, 6 hrs per night, 15 day flight) of the BACH payload to cosmic ray Fe, Si, C, N, and O with differential spectra proportional to $E^{-2.5}$ and constant composition extrapolated from lower energy data. Silicon events in panel (a) obscure some underlying iron events. Carbon, nitrogen and oxygen are shown separately in panel (b) for visibility. Results are expressed as simulated pulse heights (in mV) from two collectors (C1 and C2) given the instrument parameters and atmosphere of the PDQ-BACH flight.

Fig. 3.— Balloon Air Cherenkov (BACH) long duration balloon payload design with 250 m²-sr geometry factor. PDQ BACH consisted of the two highlighted detector assemblies and associated electronics. Centerline separation of the collectors was 2.87 meters for PDQ BACH.

Fig. 4.— Pressurized Optical Detectors (PODs) utilized by PDQ BACH.

Fig. 5.— Oscilloscope traces resulting from four triggers during the PDQ BACH flight. Traces are offset in units of 10 mV. Strong, coincident pulses in C1 and C2, along with an absence of signal in anticoincidence detectors A1 and A2, identify the event in panel (a) as resulting from an iron nucleus. The timing offset of 2.5 ns tags the event in panel (b) as a skylight fluctuation. Panel (c) illustrates a background event where a charged particle is detected in C1 and its anti A1, while a skylight fluctuation occurs in C2. In panel (d), the presence of signals in A1 and A2, and the 10 ns offset between the C1 and C2 pulses indicates a charged particle passing through both light pipes.

Fig. 6.— Flight data from PDQ BACH during the first 1.75 hrs of operation. These data may be compared to the simulation shown in Figure 2. The flight data include skylight and charged particle backgrounds, whereas the simulation contains only cosmic ray air Cherenkov events.

Fig. 7.— Determinations of the cosmic ray iron flux by other investigators compared to results from PDQ BACH. Sood (1983) pioneered the BACH technique. The JACEE determination (Asakimori et al. 1995) is a compilation of data from 12 flights. CRN (Swordy et al. 1993) was conducted on the Space Shuttle.

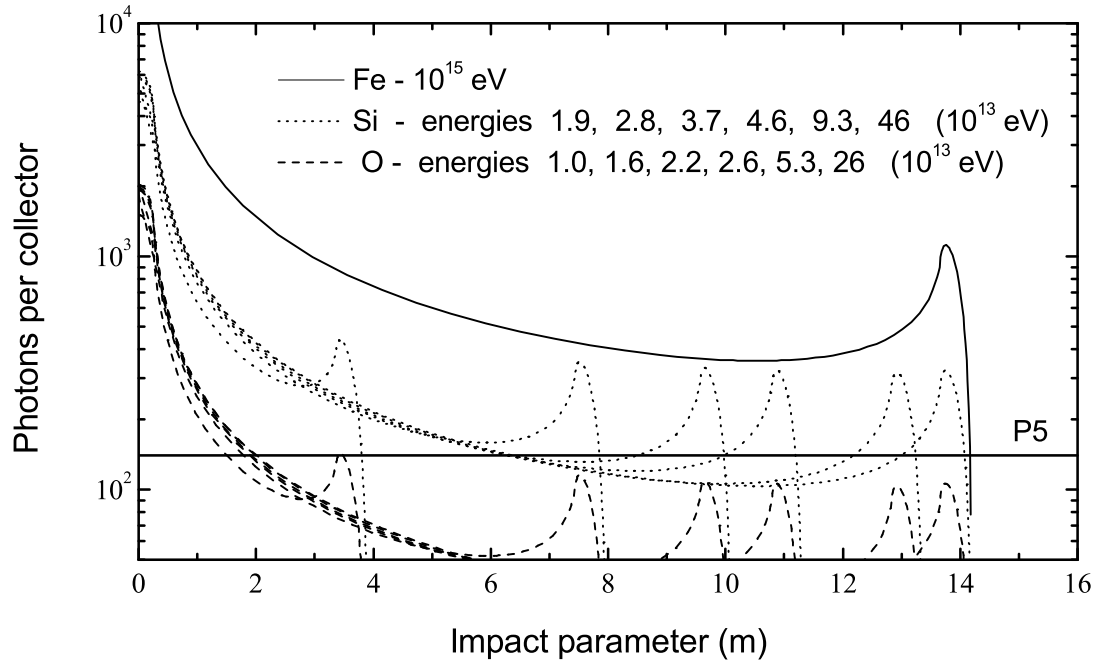


Figure 1

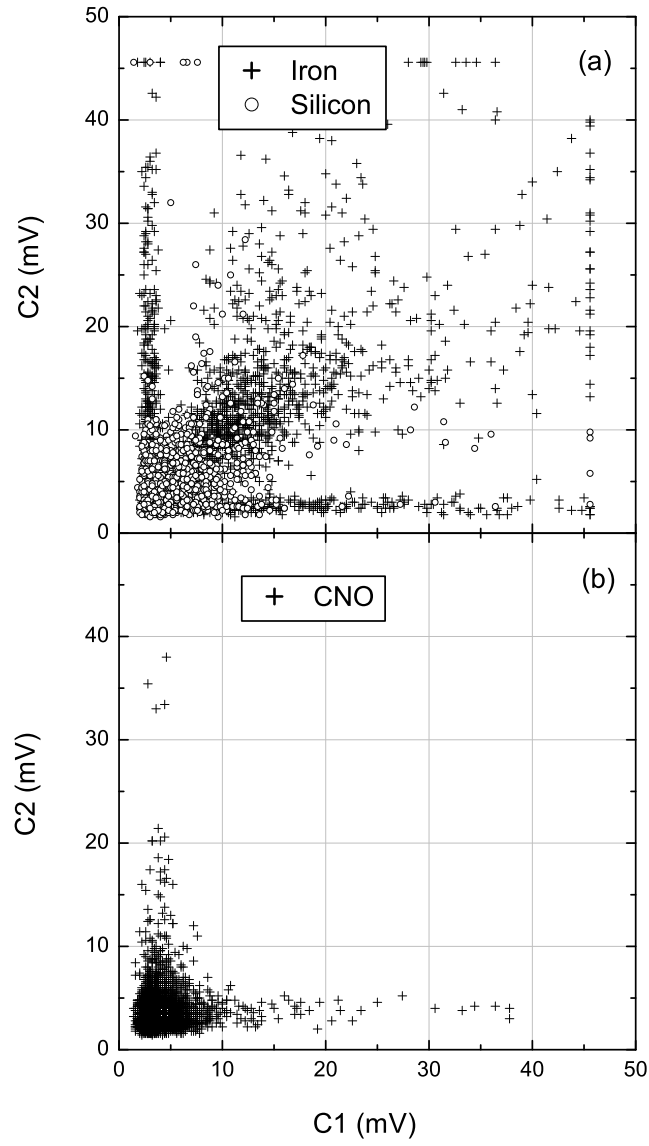


Figure 2

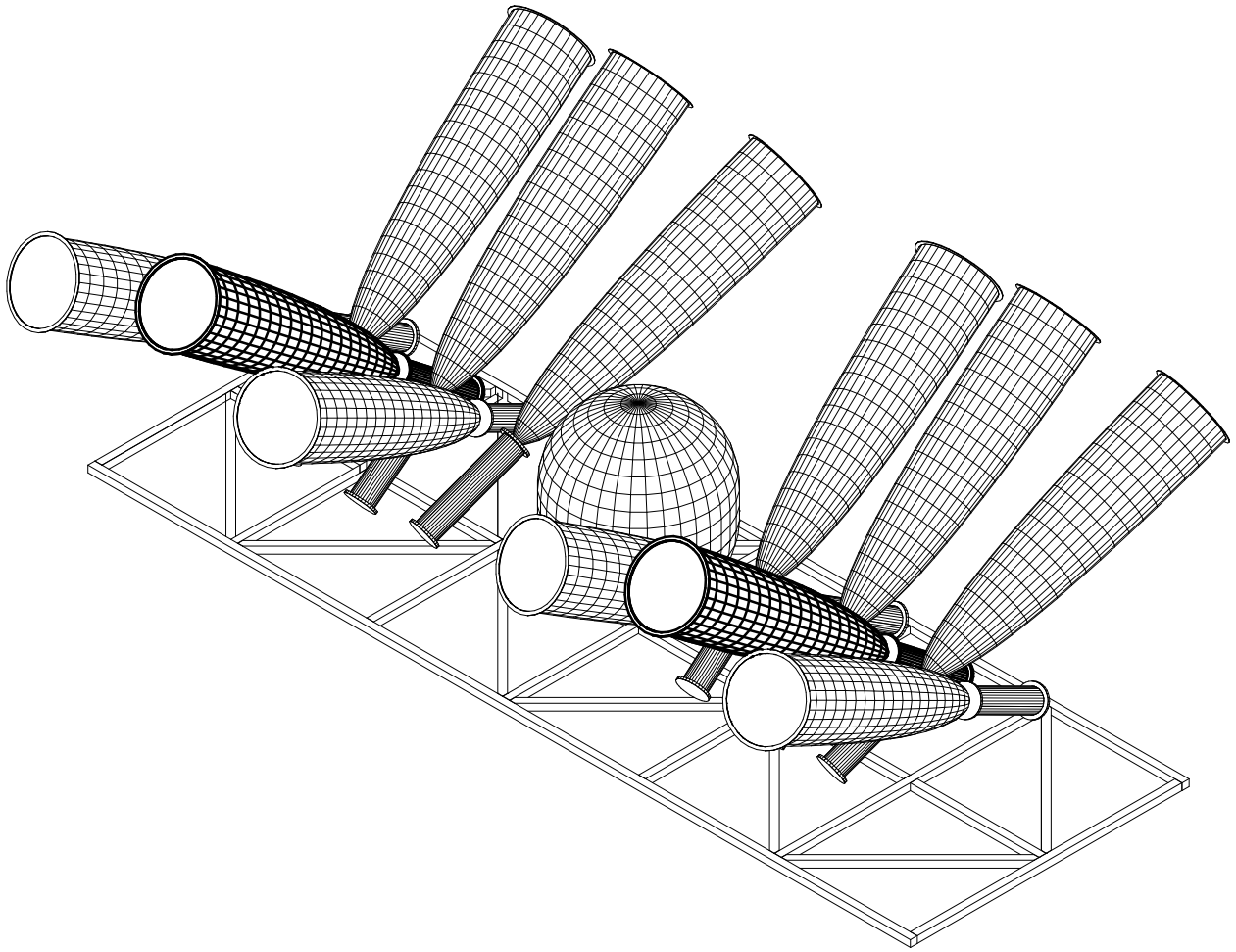


Figure 3

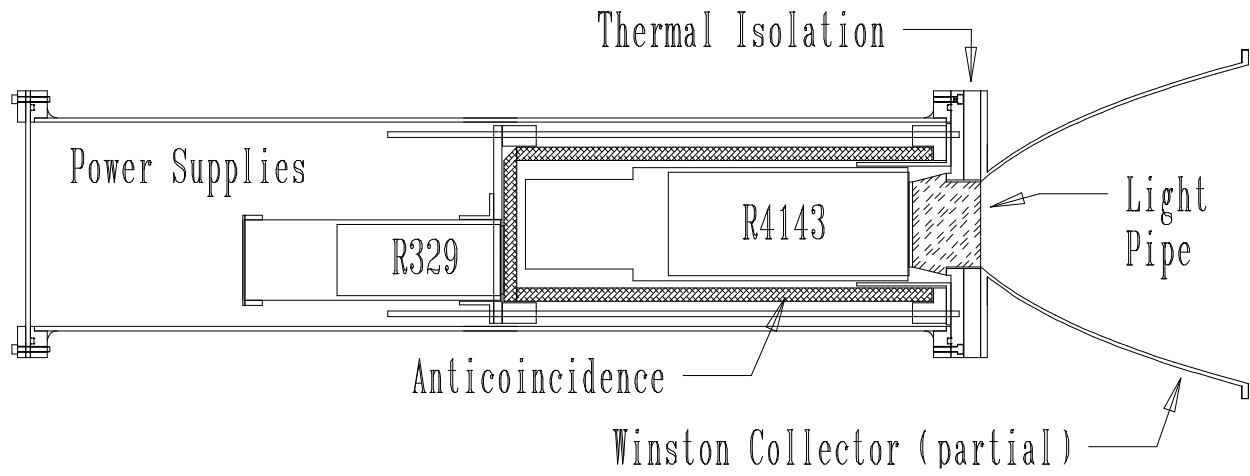


Figure 4

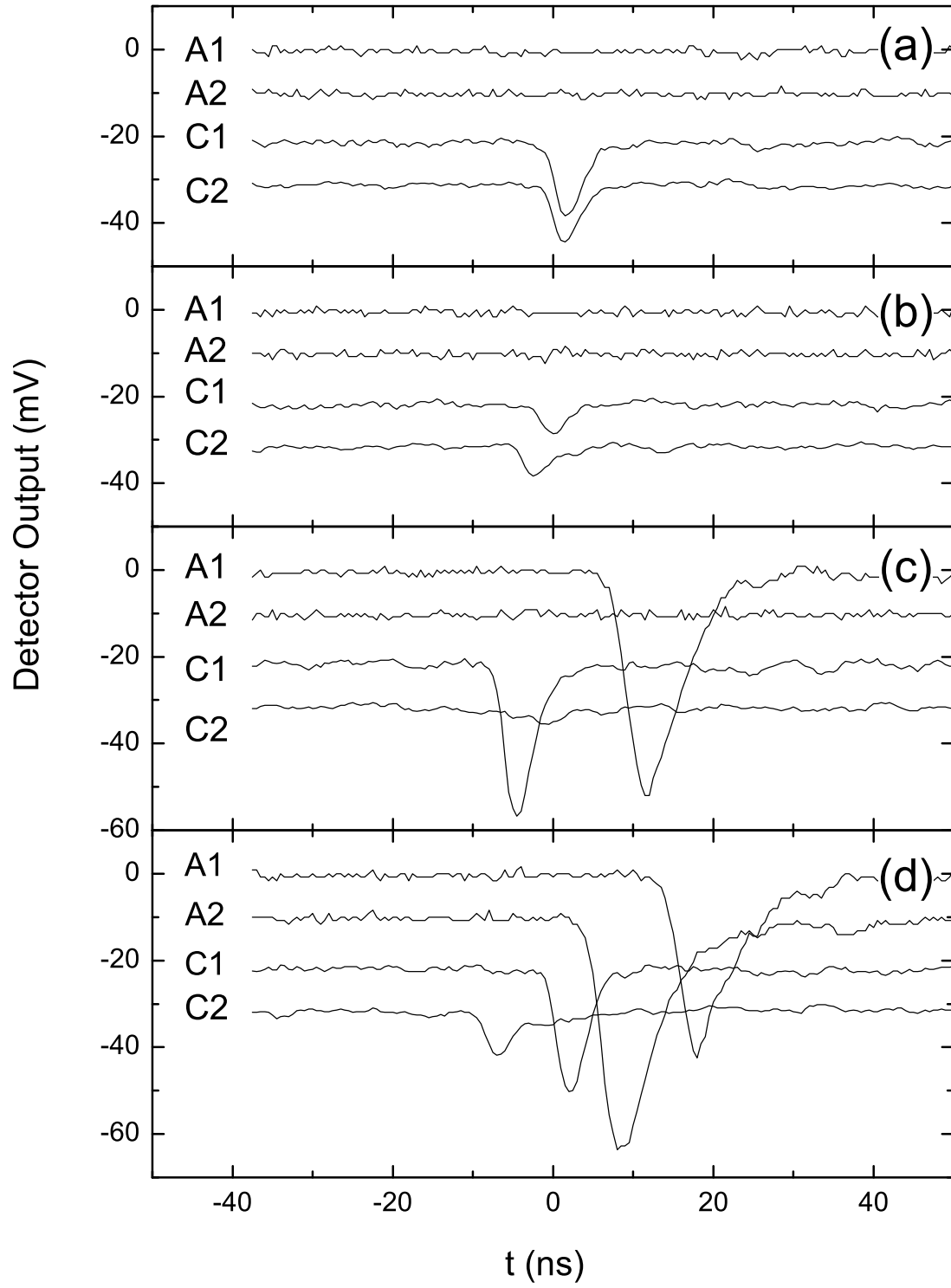
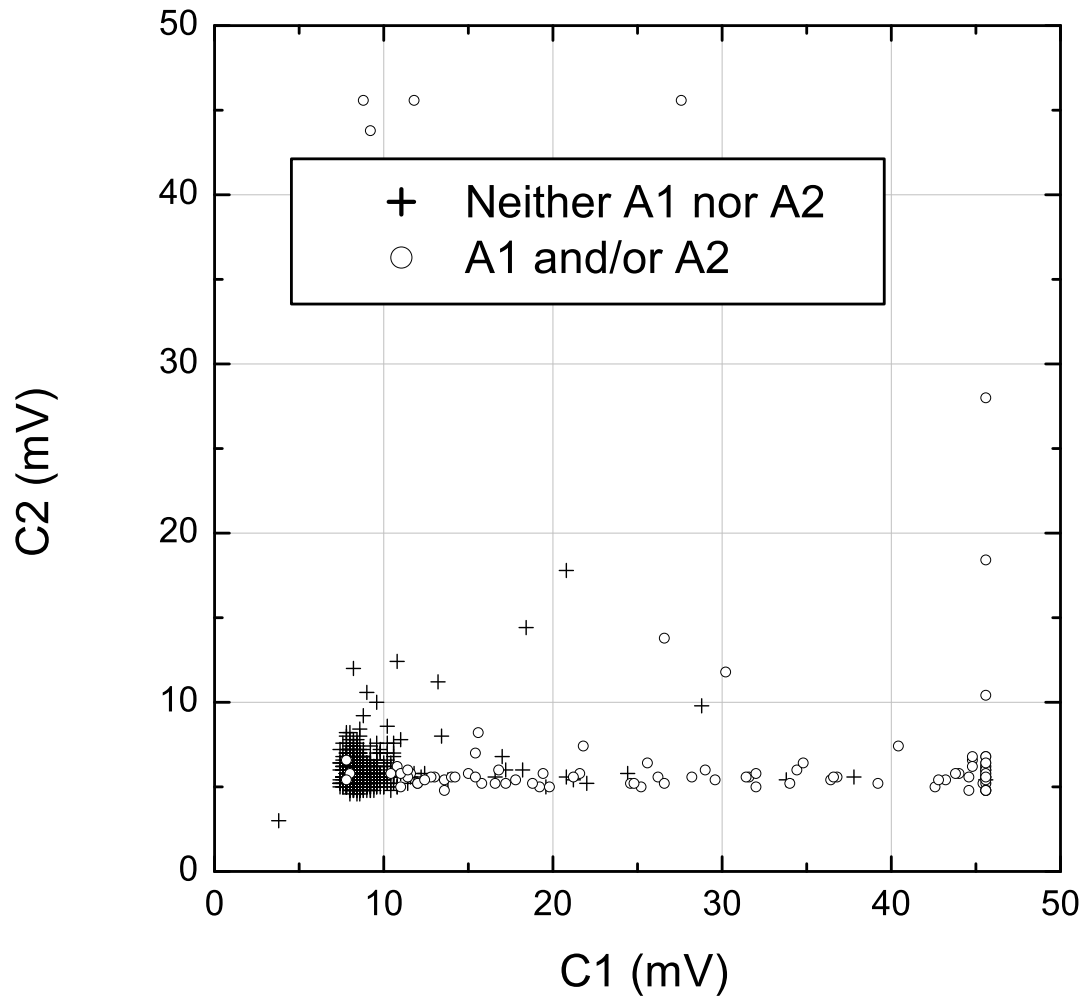


Figure 5



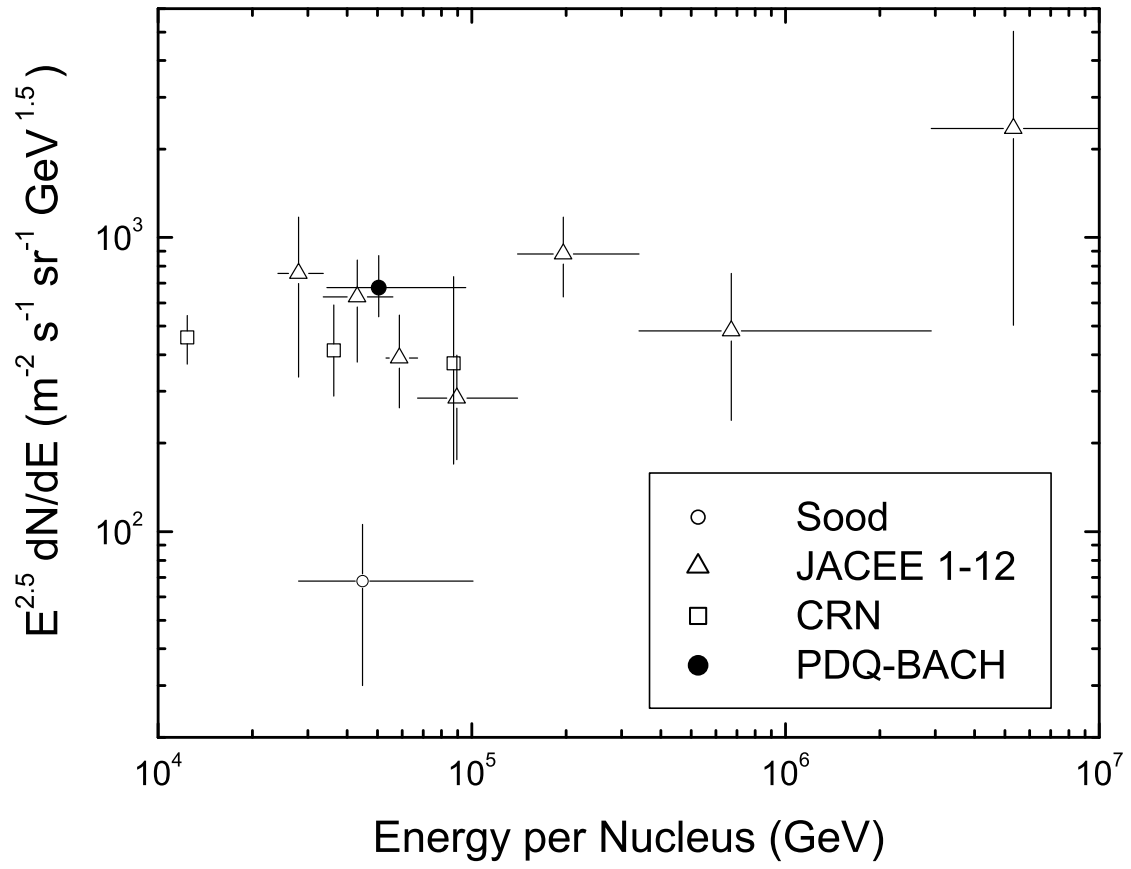


Figure 7